



**Fermi National Accelerator Laboratory**

**FERMILAB-TM-2012**

## **Fast PIN-Diode Beam Loss Monitors at Tevatron**

Vladimir Shiltsev

*Fermi National Accelerator Laboratory  
P.O. Box 500, Batavia, Illinois 60510*

July 1997

## **Disclaimer**

*This report was prepared as an account of work sponsored by an agency of the United States Government. Neither the United States Government nor any agency thereof, nor any of their employees, makes any warranty, expressed or implied, or assumes any legal liability or responsibility for the accuracy, completeness, or usefulness of any information, apparatus, product, or process disclosed, or represents that its use would not infringe privately owned rights. Reference herein to any specific commercial product, process, or service by trade name, trademark, manufacturer, or otherwise, does not necessarily constitute or imply its endorsement, recommendation, or favoring by the United States Government or any agency thereof. The views and opinions of authors expressed herein do not necessarily state or reflect those of the United States Government or any agency thereof.*

## **Distribution**

*Approved for public release; further dissemination unlimited.*

# Fast PIN-Diode Beam Loss Monitors at Tevatron

Vladimir SHILTSEV  
*Fermi National Accelerator Laboratory*  
P.O. Box 500, Batavia, Illinois 60510

July 30, 1997

## **Abstract**

The article is devoted to results of fine time structure of particle losses in Tevatron with use of fast beam loss monitors (BLM) based on PIN-diodes. An ultimate goal of the new BLMs is to distinguish losses of protons and antiprotons from neighbor bunches with 132 ns bunch spacing in the Tevatron collider upgrade. The devices studied fit well to the goal as they can recognize even seven times closer – 18.9 ns – spaced bunches' losses in the Tevatron fixed target operation regime. We have measured main characteristics of the BLM as well as studied the proton losses over 10 decades of time scale – from dozen of minutes to dozen of nanoseconds. Power spectral density of the losses is compared with spectra of the proton beam motion.

# 1 Introduction

The Tevatron collider upgrade follows several approaches to get higher luminosity. Improvement of the injection chain with Main Injector ring, an increase of the antiproton production rate and antiproton recycling in the Recycler ring, etc, all will valuably increase a number of bunches and bunch population, and the colliding proton and antiproton beam intensities as a whole [1, 2].

Besides general expectation of higher beam losses with higher beam intensities due to beam-gas collisions and intrabeam scattering, several issues arise caused by beam-beam forces at two interaction points (IPs, at B0 and D0 low-beta regions) and additional  $2 \times (N_b - 1) \sim 200-300$  parasitic crossings of proton and antiproton bunches. The design value of the total tune shift for antiprotons (pbars) is about maximum experimentally observed value for proton colliders  $\xi \approx 0.025$ . Thus, as the tune spread of the same value, one may expect an increase of the particle losses due to crossing of higher order lattice resonances.

Then, in order to achieve sufficient beam-beam separation outside IPs, a crossing angle of about 200 microradian between proton and antiproton orbits at the main interaction points is proposed. The crossing angle leads to synchrotron coupling, additional resonances, beam blow-up, particle losses and luminosity degradation [3].

Another beam-beam induced effect is the betatron tunes variation along the bunch train (composition of the “head-on” and long-range electromagnetic interaction and due to unequal proton bunch intensities) and  $x - y$  coupling due to skew component of the beam-beam kick [2]. The maximum bunch-to-bunch spread  $\Delta\nu_{max}$  of the vertical and horizontal tunes is estimated to be about 0.003 during the Tevatron Run II and about 0.01 in TEV33. Thus, the lifetime becomes dependent on the bunch position, e.g. the most severe effects and, therefore, higher losses, are expected for the bunches near the abort gap and injection gaps in the beams (so called PACKMAN effect). As several ways to avoid the effect are under consideration (see, e.g. [4]), there is a need in a beam loss monitor which can distinguish particles lost from different bunches even when the bunch spacing is 132 ns. Such monitors could be also considered as an ideal candidate for loss diagnostics in future multibunch machines, like 100 TeV proton-proton supercollider “Pipetron”, where the bunch spacing is of the order of hundred nanoseconds [5].

The present Tevatron loss monitor system [6] relies on 216 Argon filled glass sealed coaxial ionization chambers. Most are positioned adjacent to each superconducting quadrupole. Linear dynamic range of the ionization chamber is about  $10^4$  (usable of about  $10^5$ ). There was no need in a bunch-by-bunch loss monitoring at the time of the system installation and the integration time constant was selected to match known properties of the beam-induced quench of the Tevatron superconducting dipoles, and is equal to 60 ms.

About  $10^6$  times faster PIN-diode BLMs and the first results of their application

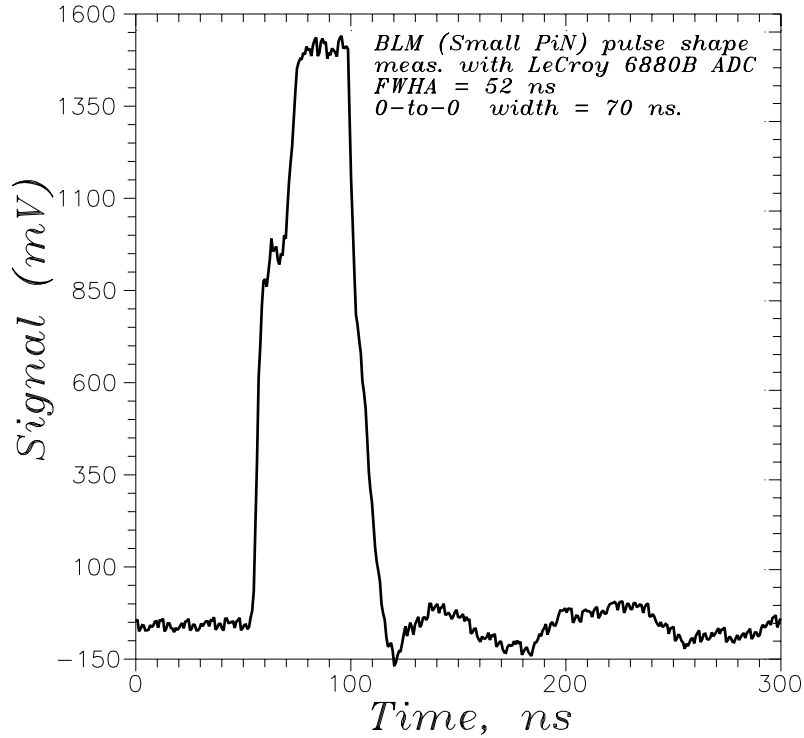


Figure 1: The output signal of the BLM with 7.34 mm<sup>2</sup> BPW34 PIN-diode from Siemens.

at the Tevatron are described in this article.

## 2 Operation, test and calibration of PIN diode BLM.

The PIN diode is essentially a  $p^+nn^+$  semiconductor structure (usually silicon based). Details of its operation can be found elsewhere [7]. The most important feature for the purpose of particle detection is enlarged depletion region (region of Si bulk without free carriers, electrons or holes, in PIN diode it is  $n$  region, also referred as  $I$ -layer), which can be as large as 300  $\mu\text{m}$  in Hamamatsu S2662-02 PIN photodiode used in our studies. Minimum ionization particles (MIPs) come through the depletion region leaving products of ionization behind, about 25,000 electrons and holes over 300  $\mu\text{m}$ . Therefore, MIPs lose energy – 3.6 eV is required to create an electron-hole pair – with a rate of  $dE/dx = 3.7 \text{ MeV}/\text{cm}$ . Thicker depletion layer is beneficial because of more pairs born, and smaller capacity which is proportional to  $(\text{diode area}/\text{depletion layer width})$ . Now, if the reverse voltage applied, then the electric field prevents the pairs recombination and separate charges effectively, and one sees current impulse. Charge collection time decreases with increased depletion voltage and is limited by velocity saturation at high fields, e.g. at extreme, in 300  $\mu\text{m}$  thick detectors with about 300 V reverse bias, electrons are collected within

about 8 ns, and holes within about 25 ns. We operate the PIN diode with 25 V bias, and the BLM output pulse width was  $\tau=56$  ns at 10% amplitude – see Fig.1.

The beam loss monitors using PIN diodes were developed in DESY [8]. In our studies we used essentially the same BLMs by BERGOZ Precision Beam Instrumentation [9] which made them smaller by using surface mounted components – the size of the monitor is  $69 \times 34 \times 18$  mm.

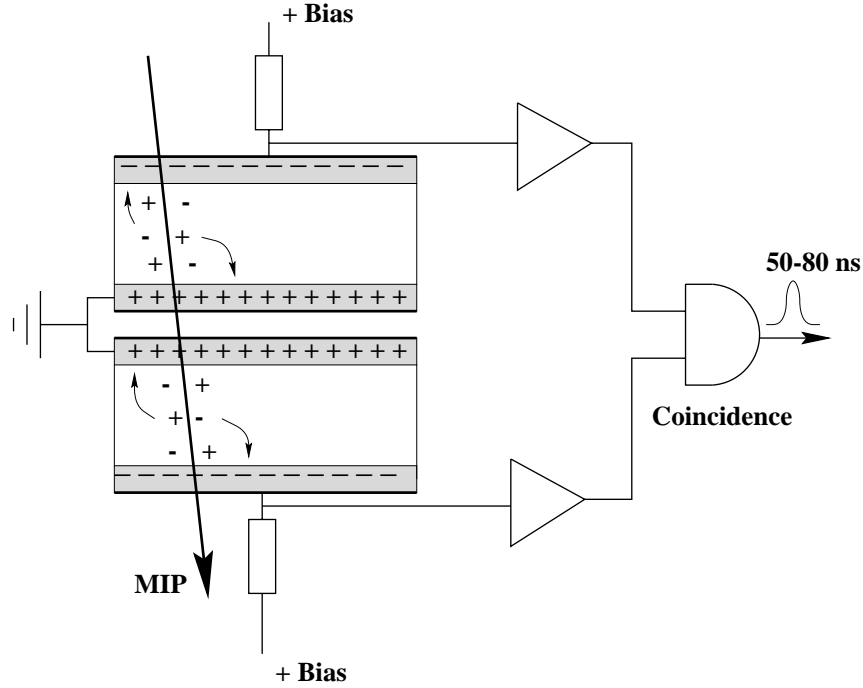


Figure 2: Scheme of the PIN-BLM operation.

The monitor consists of two reverse biased PIN-diodes mounted face-to-face. Charged particles which cross both diodes produce signals in both diodes. To reduce the electronic noise<sup>1</sup> and low-energy photon background only a coincidence signal from the two diodes is used – see the BLM layout in Fig.2. For example, a single diode spurious count rate is some kHz, while the coincidence scheme output gives less than 1 Hz. Further reduction to 0.1–0.01 Hz can be made by adjusting the discriminator threshold. Therefore, taking into account about 50ns pulse width, we get the dynamical range of the monitor of  $2 \cdot 10^8 - 2 \cdot 10^9$ .

The monitor with Siemens BPW34 PIN-diode of  $7.34 \text{ mm}^2$  area was calibrated at DESY with respect to the BLM with previously measured efficiency of  $\varepsilon_0 = 0.35 \pm 0.02$  [10]. The same Ru-106  $\beta$ -source with about  $300 \mu\text{Ci}$  activity was used for both probes. The DESY BLM covered  $2\pi$  solid angle and gave  $105.2 \pm 37.2$  counts per 10 seconds while the PIN diode in BERGOZ BLM covered only 1.27 sr of solid

<sup>1</sup>mainly produced by the diode dark current, its capacitance, and by transistors in the first amplification circuit

angle being about 2.4 mm from the source and produced  $26.0 \pm 7.9$  counts per 10 seconds. Therefore, the efficiency of the BERGOZ BLM can be estimated as  $\varepsilon_1 = \varepsilon_0 \times (1.2 \pm 0.56)$ , i.e. the same as  $\varepsilon_0$  within the error of measurements, although the latter was large.

Two BLMs equipped, one with two  $7.34 \text{ mm}^2$  BPW34 diodes from Siemens and another with  $7.5 \times 20 = 150 \text{ mm}^2$  S2662-02 photodiodes from Hamamatsu were used in our experiments at Tevatron. The electronic circuits are the same in both cases. The larger area BLM signal has a slightly different pulse shape, about 10% larger pulse width, and about 1.5-2 times larger amplitude than the smaller area PIN diode monitor (2.5-3 V on  $50 \Omega$  load with respect to 1.5-2 V). Besides +24V for reversed biasing of the diodes, the BLM requires  $\pm 5\text{V}$  power supplies for electronics.

Initial tests with Sr-90 0.5 MeV  $\beta$  source and with Ru-106 3.5 MeV  $\beta$  source have shown that in order to get well detectable count rate, the source activity has to be several dozens of  $\mu\text{Ci}$ . While the energy of the  $\beta$  particles is in the MeV range, the 0.2 mm thick copper cover over the PIN-diode causes about 10 times reduction in the count rate. For high energy particles (hundreds GeV protons) the cover does not matter. Extremely high radiation resistance of the PIN diode BLMs – they are reported to survive well irradiation of  $2 \cdot 10^8$  rad [11] – makes them very useful for accelerator applications.

### 3 PIN-BLMs at Tevatron

Particle loss studies with the PIN-BLMs were carried out from March to June 1997 when the Tevatron worked for fixed target experiments. Injection of about  $2.5 \cdot 10^{13}$  protons from the Main Ring took place at 150 GeV. The accelerator operated with some 1000 bunches at 800 GeV. Minimum bunch spacing was about 18.9 ns which is 7 times less than for TEV33 upgrade regime. The rms bunch length in Tevatron is about 1-2 ns – very small with respect to the PIN-diode pulse width. Therefore, if two or more particles, simultaneously lost from the same bunch, cross the diode area then one can see only one BLM count. It yields in maximum possible counting rate of about  $159 \times 47.7 \text{ kHz} = 7.6 \text{ MHz}$  with 132ns bunch spacing (i.e. one particle lost and detected from each of maximum 159 bunches at every turn, the revolution frequency of 47.7 kHz); and  $1/\tau \simeq 12\text{-}16 \text{ MHz}$  for 18.9ns spacing (one count per turn from every 3-4 bunches).

For our studies we attached two BLMs immediately to the vacuum chamber of the Tevatron near the end of the Sector F0, at the F11 magnet. Nearby located ionization chamber gives the radiation level there to be about  $D = 0.0005\text{-}0.0012$  rad/sec – one of the lowest values along the Tevatron. The radiation level distribution in the Tevatron during the fixed target regime is shown in Fig.3. Having the dose  $D$  one can estimate the flux of MIPs  $\Phi$  accordingly to formula:

$$\Phi = D / (dE/dx), \quad (1)$$

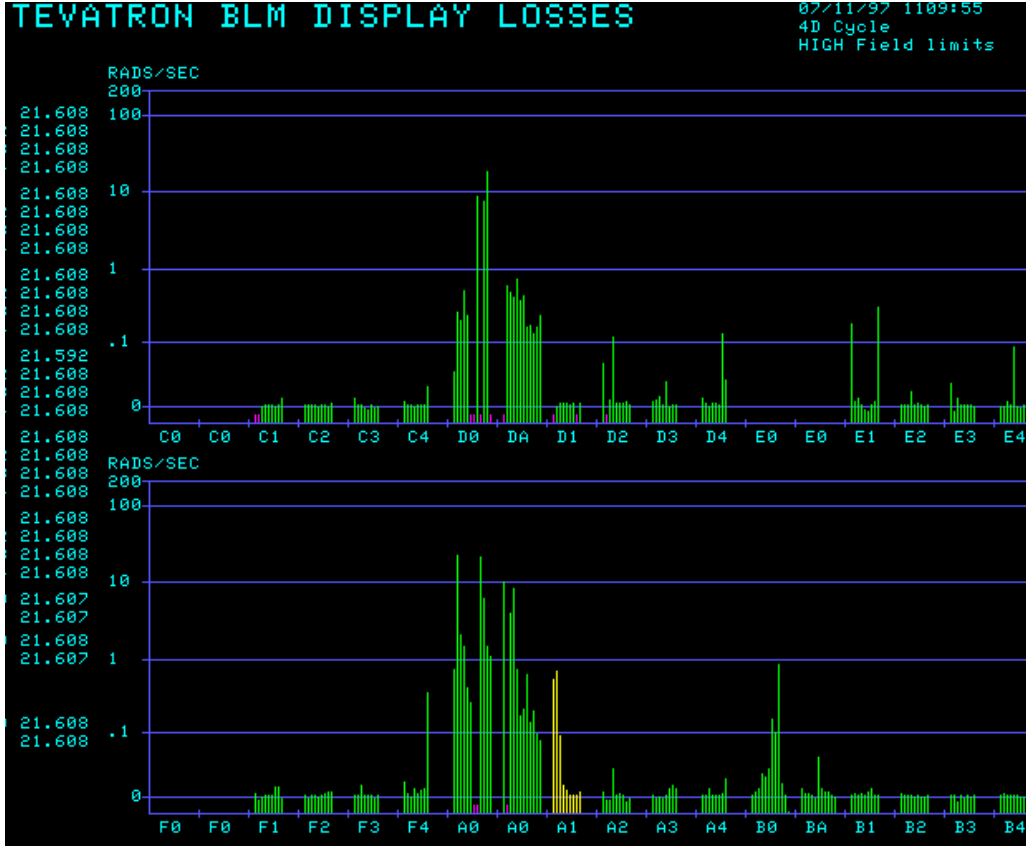


Figure 3: Radiation levels around the Tevatron ring measured with ionization chambers (courtesy of the Tevatron control room).

or  $\Phi \approx (1.25 - 3) \cdot 10^4 \text{ 1/cm}^2/\text{s}$  for  $dE/dx = 2.5 \text{ MeV}/(\text{g/cm}^2)$ .<sup>2</sup> For a monitor with  $1.5 \text{ cm}^2$  area of the PIN diode, and efficiency of 0.35, one gets the BLM count rate of  $\dot{N} = 6 - 16 \text{ kHz}$ . In fact we observed up to 6 times larger rates, probably because of a) continuously improving beam intensity, b) ionization chambers are installed not so close to the vacuum chamber and shielded by the magnet iron that reduces the flux:

$$\Phi \propto \frac{1}{r} \exp(-d/\lambda) \quad (2)$$

where  $r$  is radius from the beam orbit,  $d$  is the metal thickness, and  $\lambda \sim 15 \text{ cm}$  is the interaction length in iron.

About 40 m long coaxial cables from the Tevatron RF equipment room to the tunnel are used to supply the BLMs with  $\pm 5\text{V}$  and  $+25\text{V}$ , and for transmitting outputs of the BLMs and nearby located strip-line BPM to a data acquisition system.

<sup>2</sup>here we used an definition  $1 \text{ rad/sec} = 6.24 \cdot 10^7 \text{ MeV/g/s}$

### 3.1 Data acquisition

Scheme of the CAMAC-based data acquisition system is shown in Fig.4. Analog signals from the two PIN-BLMs (+1.5–2.5 V) go to LeCroy 2323A gate generator which works as a discriminator with variable thresholds and forms two NIM level outputs of 50 ns each. These signals go to the second LeCroy 2323A which produces the outputs as long as the external gate signal is asserted. The gate signal is synchronized with the Tevatron 7.57 MHz RF clock provided by Beam Clock/Timer module 279. Its duration is variable from 50 ns to 21  $\mu$ s (the Tevatron revolution period), and its delay with respect to AA synchronization mark is controlled by computer with a minimum step of 1/4 ns. If the signals pass the gate, then they are counted by LeCroy 2551 scaler.

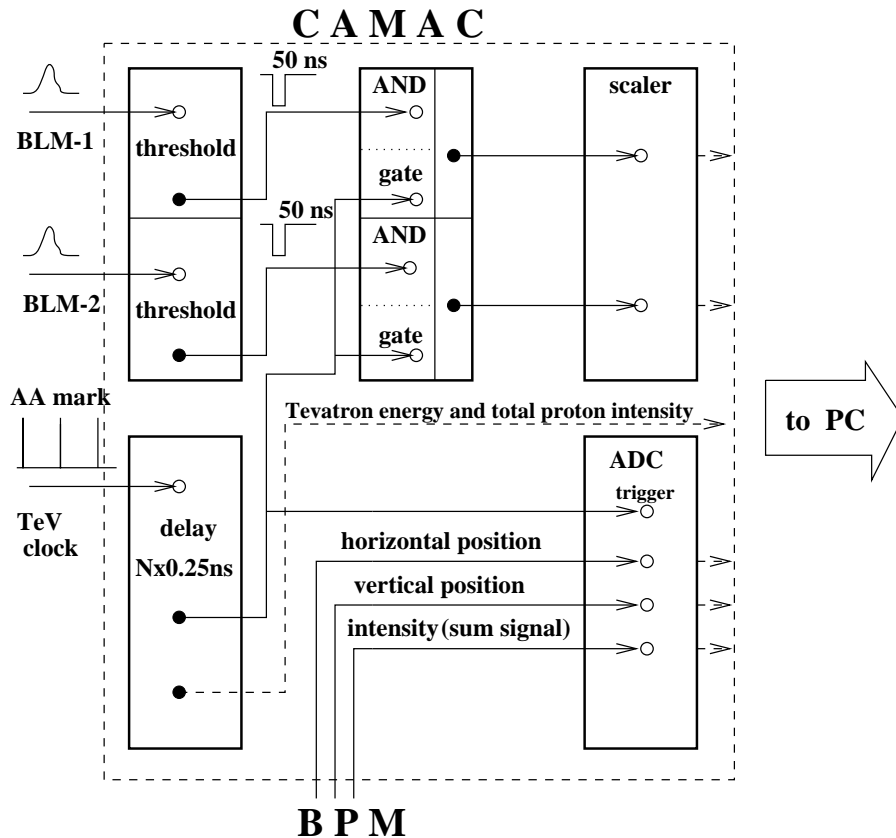


Figure 4: Scheme of the data acquisition used in the beam loss studies.

Other information we used is the proton energy (proportional to the Tevatron dipole current) and total proton intensity – these numbers are available in digital form with use of MDAT receiver module 169. ADC QD 808 triggered by the same gate signal as for BLMs, is used for digitizing analogous signals from the BPM: horizontal orbit position, vertical orbit position and sum signal proportional to the beam current. Analog electronics of the strip-line BPM occupies a separate VME crate and has a 5 MHz frequency band.

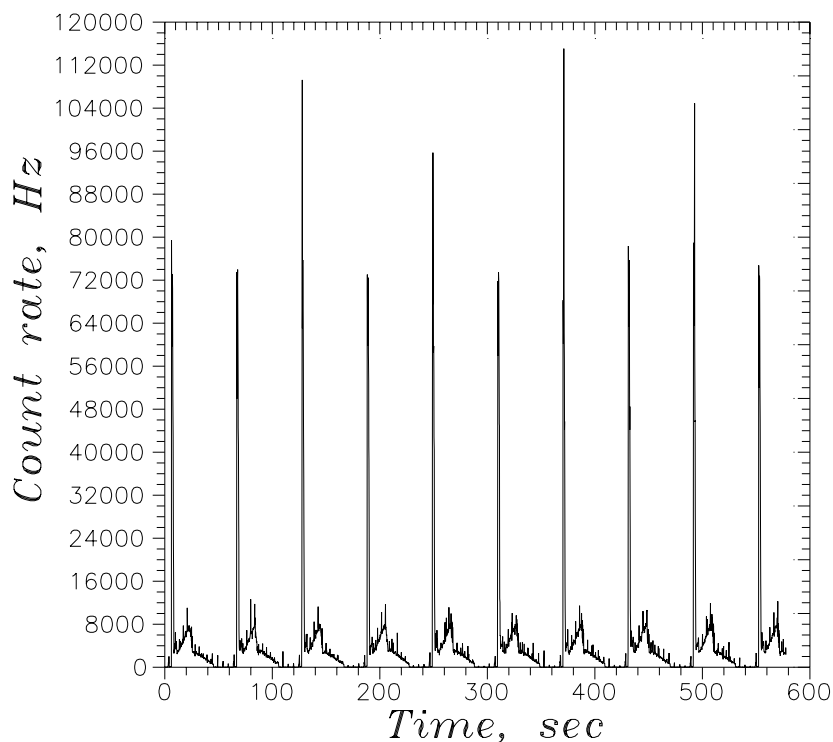


Figure 5: The BLM count rate over several cycles of acceleration in Tevatron.

All information channels from the CAMAC crate are available in a personal IBM PC/AT 386 computer through C1000 crate-controller and a parallel PC-CAMAC interface card.

## 4 Results

### 4.1 Longer time scales

Fig.5 presents the PIN-BLM count rate in Tevatron over a 10 minute time scale. The gate width 1s full revolution turn, i.e. losses from all bunches are taken into account. The loss rate is averaged over regular 100 ms intervals. The rate is almost periodic with a period of 60 sec – the Tevatron fixed target cycle period. Fig.6 shows the first of the cycles in Fig. 5 in more detail over 60 seconds. Proton energy (calculated via the SC dipole current) and intensity are presented by dashed line and thick solid line, correspondingly. About  $2.8 \cdot 10^{13}$  are injected from the Main Ring at 150 GeV (at 6 sec in Fig.6) then they are accelerated to 800 GeV within 15 sec (over so called "parabola" – as the energy changes quadratically in time) without substantial change in the beam intensity. After reaching the top energy, the beam is extracted in five steps of fast extraction to one third of initial intensity, and then slow extraction takes

place over 20 sec. After finishing the extraction, the current in the dipoles goes down and the cycle repeats.

The BLM count rate is very high over the first few seconds after injection, probably caused by imperfections like non-flat kicker pulse top, remaining betatron oscillations after injection, etc. It is then somehow stabilized at the beginning of the "parabola" and grows with the energy because each lost proton give birth to a number of secondary particles which still can ionize the PIN-diode depletion region bulk. That number is approximately proportional to the incident proton energy. During the slow extraction, the count rate decreases as the total proton current goes down. Over all the cycle, one can see some dozen of smaller and sharp peaks in the loss rate with a period of about 4 sec, which is equal to the Main Ring injection period. These peaks can be explained by injection losses in the MR which is located in the same tunnel over the Tevatron magnets.

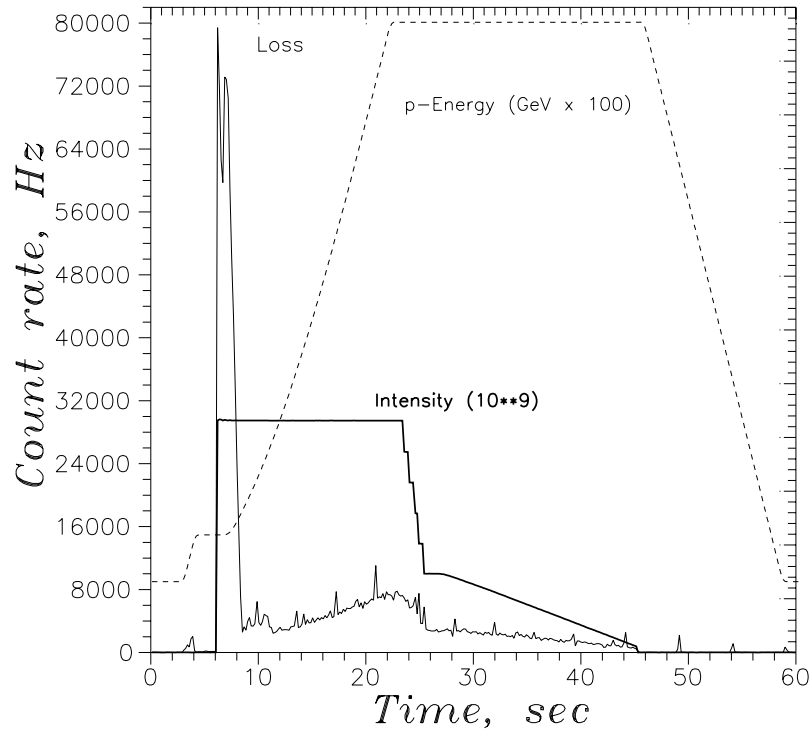


Figure 6: The BLM count rate (thin line), proton beam intensity (thick solid line) and proton energy (dashed line) over one cycle of acceleration in Tevatron.

In Fig.7 we compare count rates from two BLMs: one with large area PIN-diode and another with smaller one. One can see that they show the same temporal behavior and are different only in scale. At top energy, the monitor calibration constants are 49 counts of BLM#1 per  $10^9$  lost protons and 513 counts of the BLM#2 per  $10^9$  lost protons. The difference factor of about 10.5 is twice smaller than the ratio of

the diode areas  $20.4 = 150 \text{ mm}^2 / 7.34 \text{ mm}^2$  – probably because the probes are not located in the same point. Instead, one of them (larger area BLM#2) is set on the top of the vacuum chamber, while the other one (smaller area BLM#1) is attached to the outer side. Due to non-zero dispersion and collimators, the losses are not supposed to be equal over the azimuth, although the issue needs further experimental studies.

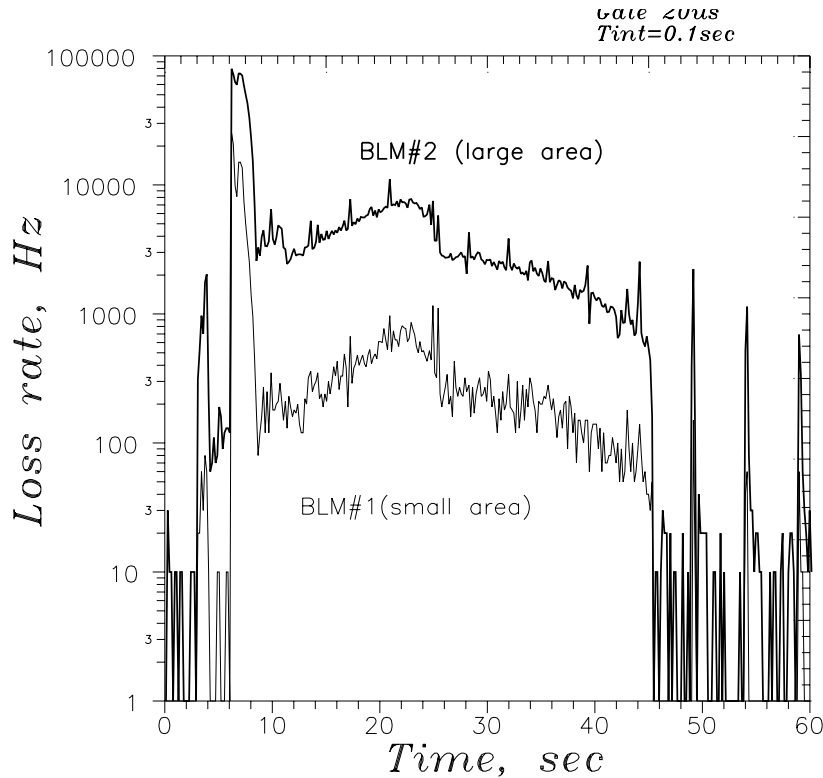


Figure 7: Count rates during the cycle of acceleration from two BLMs with different PIN-photodiode areas.

Next Fig.8 demonstrates dependence of the BLM count rate on the bias voltage. The reverse bias was set to be equal to 24V, 20V, 16V, 12V, 8V, 4V and 3V at seven consequent cycles. The beam intensity is almost the same for all cycles. One can see that the count rate varies slowly if bias goes down from 24V to 16V, but drops significantly if the voltage is 8V and less.

Looking in more detail (another factor of 1/10 in time) one can observe the time structure of losses during fast extraction as is shown in Fig.9 (thick line - for loss rate, thin line - for the horizontal orbit). The horizontal orbit is measured by the BPM in a frequency band of 300 Hz and its maximum deflection in Fig.9 corresponds to approximately 1 mm movement. In this measurements only, the BLM signals are transformed from positive 60-ns pulses to negative NIM pulses  $10 \mu\text{s}$  long, which are further integrated by an amplifier with 100 Hz bandwidth and sent to the same ADC as used for the BLM signals. The beam position is disturbed five

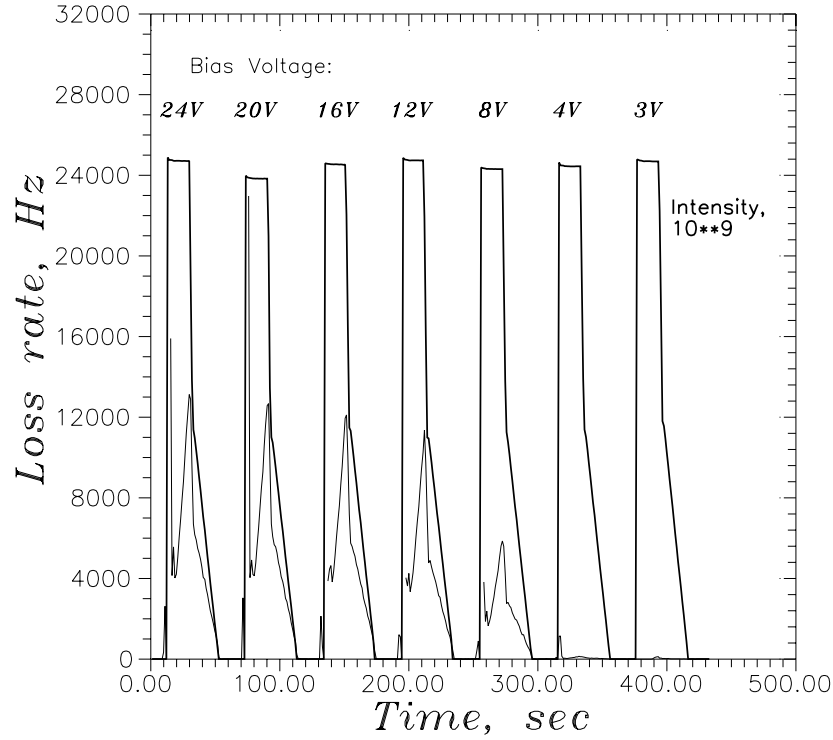


Figure 8: The PIN-BLM count rate with different reverse bias voltages. The proton intensity (thick line) is about the same over seven cycles.

times by extraction kicks, and, correspondingly, there are five peaks in the BLM signal. Aside from periods of strong beam disturbances, no regular structure is seen in losses which look like a noise.

It is clearly seen in the power spectral densities of the loss and BLM signals measured during the "parabola" (acceleration) – see Fig.10. The orbit spectrum demonstrates many peaks at 4.5Hz, 7Hz, 9.5Hz, while the only not-well recognizable peak at about 9.5Hz is seen in the loss spectrum. Broad and continuous spectrum is a specific feature of noisy processes. Note, that during the the fixed target of operation Tevatron, the beam is very unstable. It does not live for a long time under the same condition, its losses are higher and not stationary. In the collider regime with hours of stable operation, one may expect more stationary and, generally speaking, smaller losses which now can carry information about routine beam orbit disturbances. This information can be used for their identifications via analysis of the peaks in the spectra as it is done at HERA [12, 13].

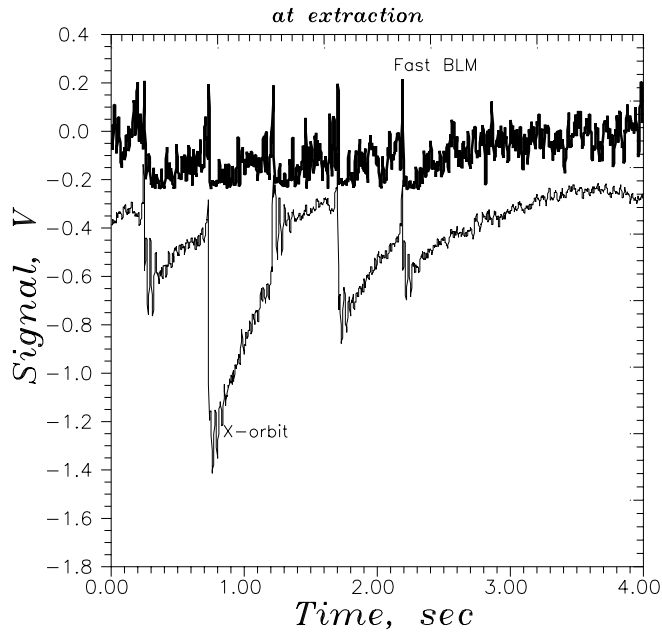


Figure 9: 4-sec time record of the horizontal orbit signal from BPM and the BLM output integrated with  $\tau = 1/f_0 = 1/300\text{Hz}=3.3$  ms (thick solid line) during fast extraction from Tevatron.

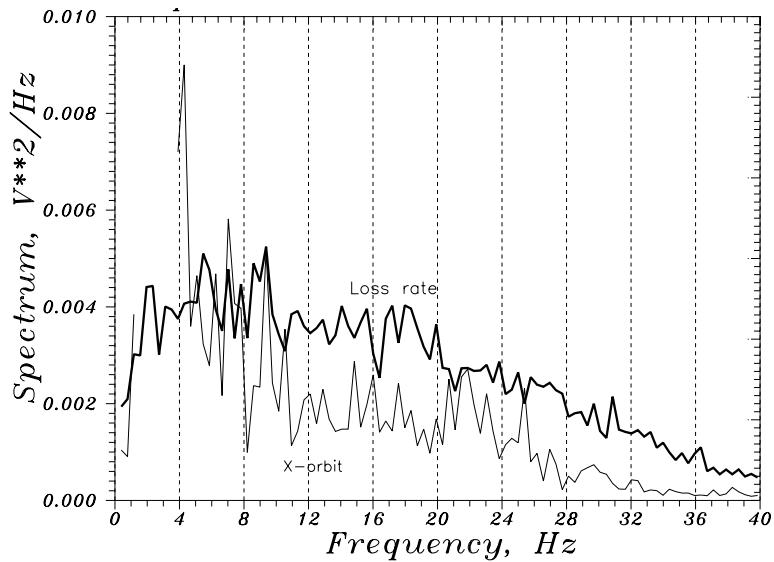


Figure 10: Power spectral densities (a.u.) of the BLM signal (thick solid line) and the horizontal orbit signal (thin line) measured during acceleration of protons from 225 GeV to 800 GeV (at “parabola”).

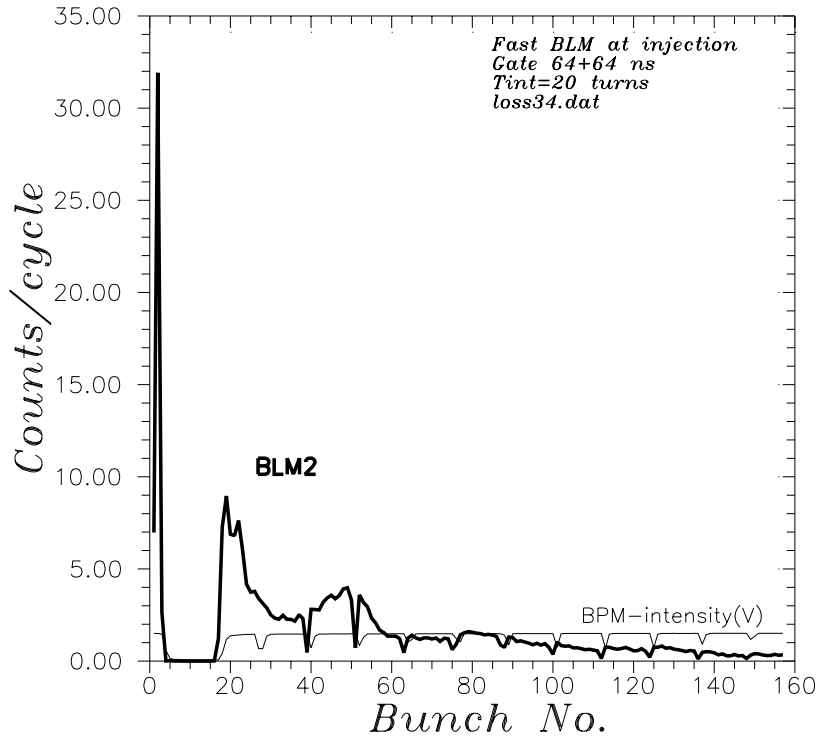


Figure 11: Distribution of losses over the proton beam at the injection energy. Thin line shows the proton intensity.

## 4.2 One-turn and one-bunch time scales

Now we consider how the PIN-BLM count rate varies over the whole bunch train of the Tevatron. Fig.11 shows the count rate measured during the first few seconds after the injection vs time delay with respect to the gap. The step in the delay time is 132 ns – every 7th RF bucket – and as it is supposed to be a bunch spacing in TEV33, we counted the time in Fig.11 as "bunch number"  $N$  from 0 to 159, although the real number of bunches in Tevatron is about 1000 in the fixed target regime.

The procedure of the measurement is as following: first, the BLM signals are counted by scaler only if a) the beam energy is in the interval from 150 GeV to 225 GeV, i.e. during the first few seconds after the injection; b) the counts appear at the time interval of  $64+64=128$  ns starting the chosen delay  $N \times 132$  ns with respect to the AA synchronization mark. The scaler counts over 20 turns of the Tevatron (0.42 ms), then the computer saves the number of the counts in the memory, gets the ADC reading of the BPM sum signal proportional to the proton charge (ADC is triggered by the same synchronization signal as the scaler gate), saves it too, and changes the synchronization from  $N$  to  $N + 1$ , etc. The data are averaged over many cycles of the Tevatron (for the particular data presented in Fig.11, the number of cycles is 434 – about 7 hours of integration).

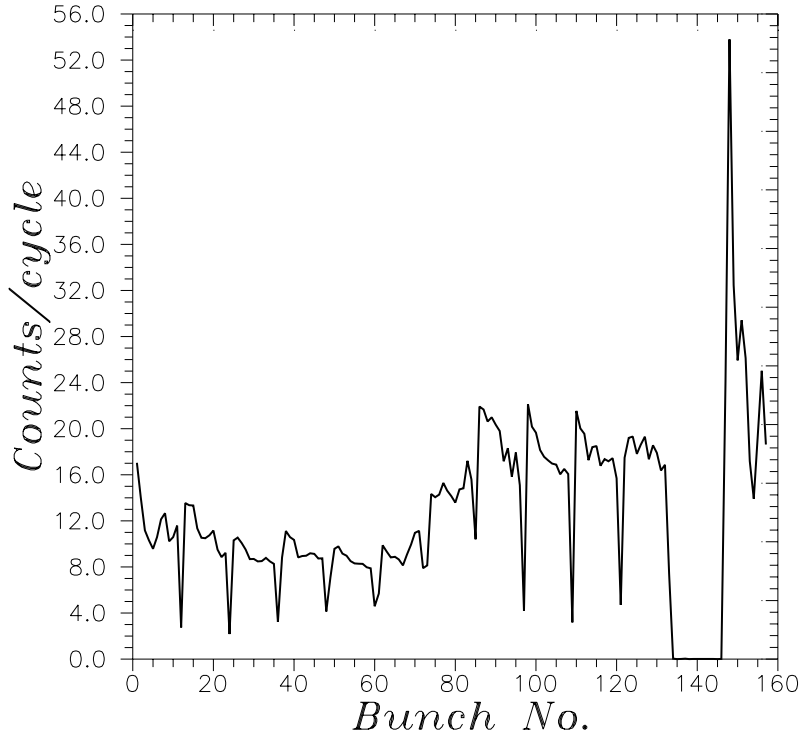


Figure 12: Distribution of losses over the proton beam at injection. Synchronization is changed from what presented in Fig.11.

In the same Figure one can see the proton intensity (thin line) which clearly demonstrates that there is about  $2 \mu\text{s}$  long abort gap in the beam, and there are twelve batches (84 bunches in each) with smaller  $\sim 100 \text{ ns}$  long gaps in between them. These short gaps are not seen as a full 100% drop in the intensity plot because of the limited frequency band of the BPM electronics and the ADC module electronics. The proton intensity does not vary too much over the beam, while the count rate varies significantly. First of all there is a huge increase of losses near the abort gap (although there are no losses during the gap time). Then, the count rate emphasize small inter-batch gaps, decreases with  $N$  and has additional broad peak at  $N = 40 - 60$ . Initially there was the idea that the smooth decrease of the count rate is an artifact of the measurements because the loss rate rapidly goes down after injection and we make one cycle of the measurements over rather long interval of  $159 \times 0.42 \text{ ms} = 67 \text{ ms}$ . Therefore, the losses at  $N = 159$  always must be the smallest, while the count rate at  $N = 1$  (beginning of the measurements' cycle) will be the biggest one. This consideration was not confirmed – e.g. in Fig.12 we present the count rate over the beam at injection but the synchronization is shifted on 130 "bunches" (and the abort gap takes place now at  $N = 134$ ). One can see that still losses are larger near the gap, but there is no continuous decrease of loss rate with  $N$ . In opposite, one half of the beam  $N = 70 - 130$  loses about twice particles then

the other  $N = 1 - 70$ . Note, that data presented in Fig.11 and Fig.12 are obtained at different times when the operation conditions were not the same, e.g. injected beam intensities were about  $1.6 \cdot 10^{13}$  and  $2.4 \cdot 10^{13}$ , correspondingly.

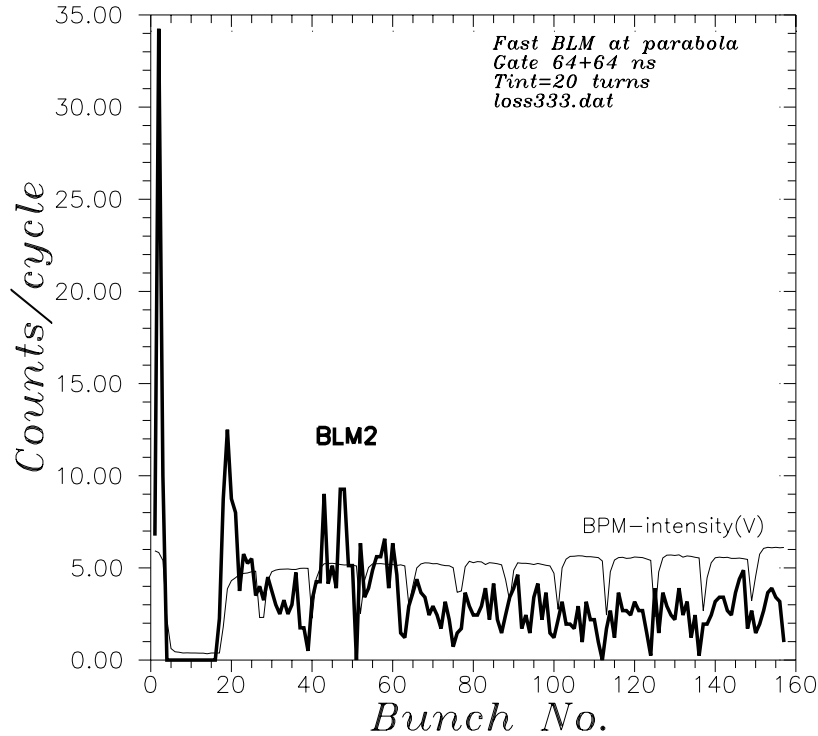


Figure 13: Distribution of losses over the proton beam during acceleration (at “parabola”).

The beam loss rate at the “parabola” (Fig.13) looks very similar to the injection one – compare with Fig.11. Distribution of losses over the beam at the top energy is very different (see Fig.14): first, the count rate is much less than at the injection and “parabola”, then, there are three huge peaks corresponding to moments of fast extraction (see thick line in Fig.14). Proton losses at slow extraction are distributed almost uniformly over the beam (see thin line in Fig.14), and they are proportional to the intensity as it is presented in Fig.15.

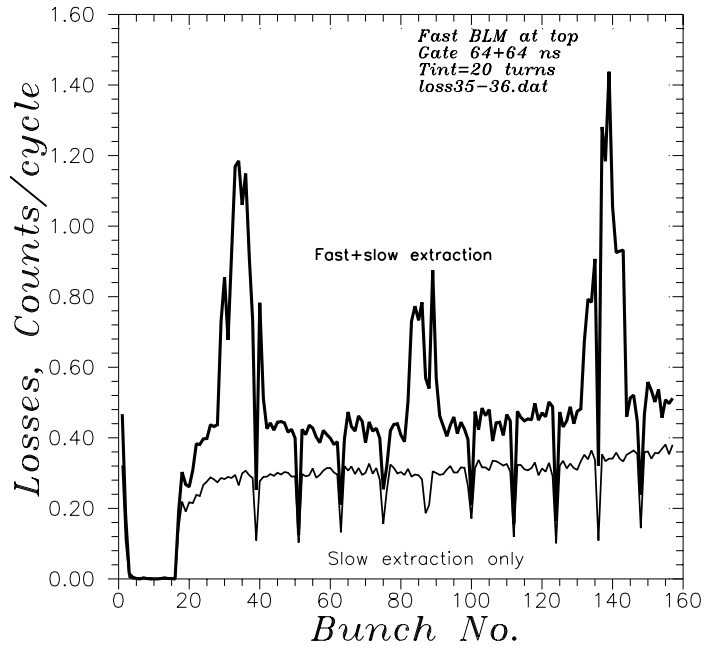


Figure 14: Distribution of proton losses over the Tevatron revolution period at 800 GeV. Thick line – the fast and slow extraction; thin line – slow extraction only.

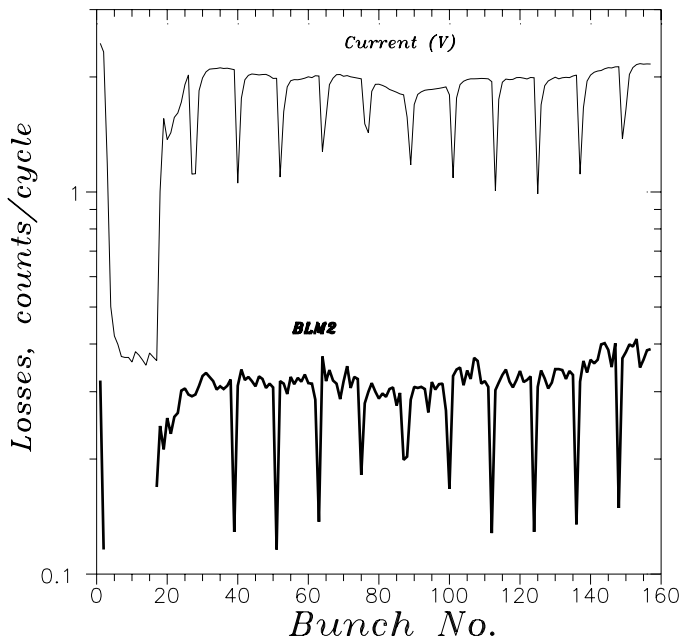


Figure 15: Distribution of proton losses over the Tevatron revolution period during slow extraction at 800 GeV. Thin line is for proton intensity.

Next step of our studies is to measure loss distribution in more detail. We performed a scan of a 800 ns long part of the Tevatron beam with 2 ns step starting from "bunch"  $N = 47$  in Fig.11, 13-15 ( $N = 31$  in Fig.12). Counting of pulses took place over the whole acceleration cycle of the Tevatron. The result is presented in Fig.16. The most remarkable feature in this Figure is the gap between two batches. One can see that the gap width is approximately 130 ns although the edges of the gap are smeared because of the gate width of  $50+50=100$  ns. Several regions of enhanced losses (around 4170 ns, 4410 ns, 4530 ns and 4850 ns) are due to larger losses at the fast extraction (see below). Small periodic variation of the count rate corresponds to 18.9 ns bunch spacing. This modulation depth of these 18.9 ns variation is rather small because the gate width (the dead time of the PIN-BLM plus the gate width for the scaler) is about five times the bunch spacing.

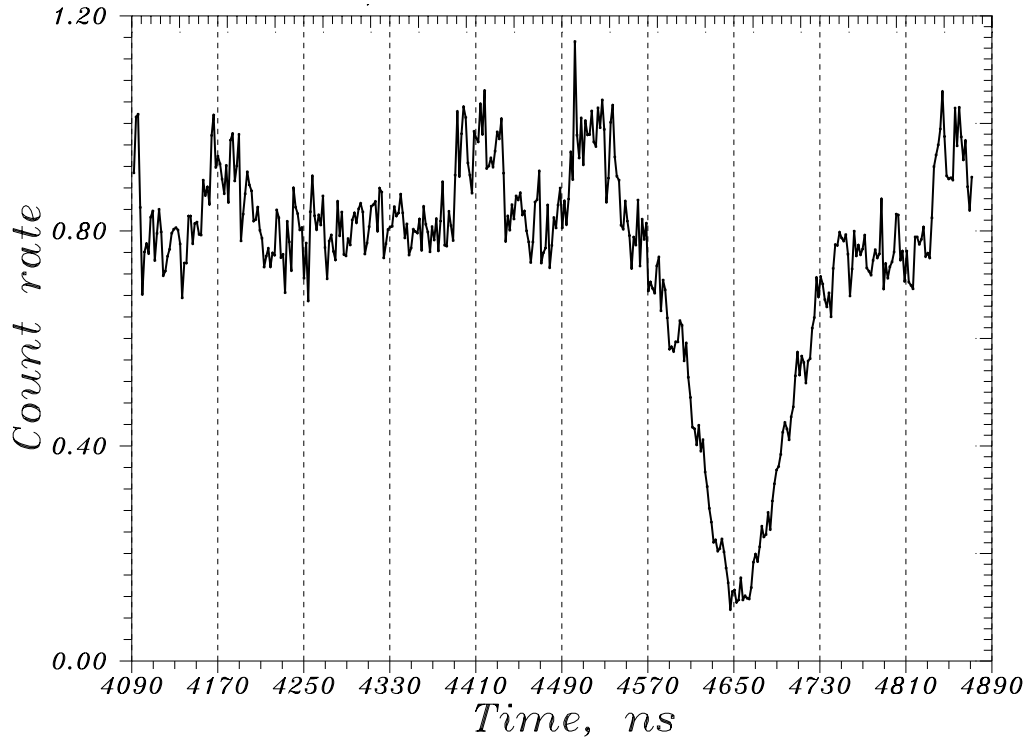


Figure 16: Losses of particular 0.8  $\mu$ s long part of the proton beam, integrated over the whole cycle of acceleration.

The bunch structure of the proton losses at injection is clearly seen in Fig.17 where we made the scan with 100 ns gate over 100 ns starting with "bunch" #57 (see Fig.11) and with a step of 1 ns. To obtain low statistical noises with about 70,000 counts in every bin we performed integration over 5881 cycles of the Tevatron (more than 4 days of operation). The value presented in Fig.15 is an average over these cycles. Now the bunch-to-bunch modulation with period of some 19 ns is clearly seen. As noted above, the modulation can not be deeper because of the limited gate width.

Indeed, assume that the lost particles come from 1-2 ns long bunches, then the factual picture of the losses  $f(t)$  looks as it shown in the bottom plot of Fig.18. The BLM and the scaler gate serve as an effective window for integration  $W(t)$  (presented by marked line in Fig.18) about 100 ns long, and the measured loss signal  $Loss(t)$  is essentially convolution of the input signal and the window:

$$Loss(t) \propto \int_{-\infty}^{+\infty} W(t') \cdot f(t' - t) dt \quad (3)$$

The resulting output is shown by dashed line which looks much like the experimentally measured data (upper solid line in Fig.18, the same as in Fig.17). For 132 ns bunch spacing in TEV33 we expect the bunch structure will be seen with full 100% deep modulation.

If we compare the losses which take place for the same bunches during the acceleration process (at "parabola) from 225 GeV to 800 GeV, then we get the picture shown in Fig.19. Although the count rate is many times smaller and the statistical error is larger than at the injection, the bunches are clearly seen again. Finally, the losses of same bunches at the top energy of 800 GeV are presented in Fig.20. The loss distribution looks different to what is shown in Figs.17,19, because of five peaks in the count rate. We found that these peaks are due to five steps of fast extraction. They always appear at the same moment of time because the extraction and the scaler gating are both synchronized to the same Tevatron clock. Locations of these peaks depend on the number of the time scan steps (e.g. 400 in Figs. 19, 20 and 100 in Fig.17) while the positions of the bunches are always the same.

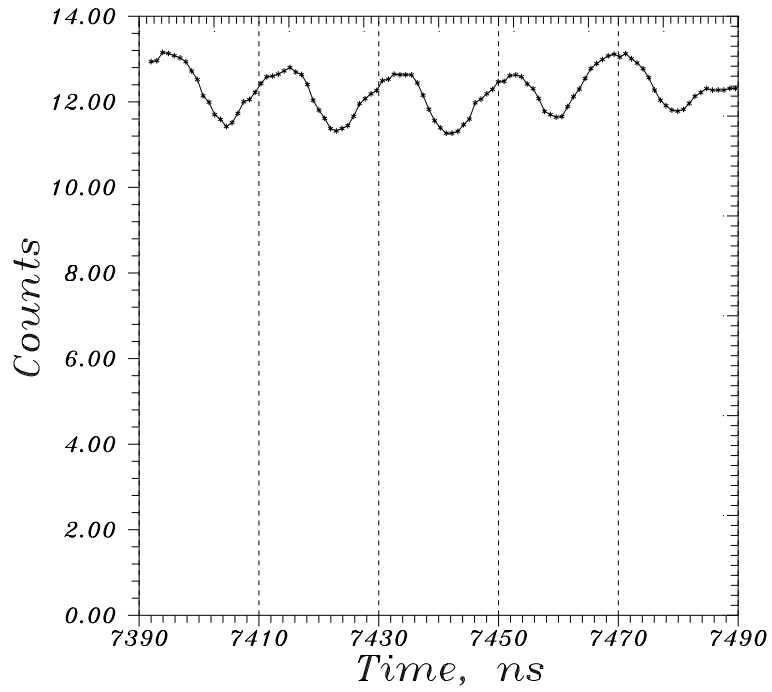


Figure 17: Proton losses of several bunches at injection.

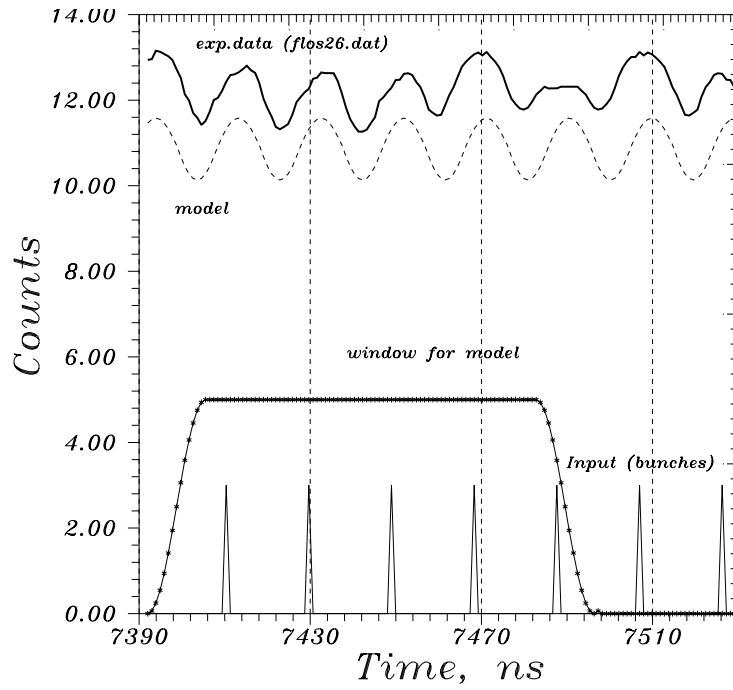


Figure 18: The same as in Fig.17 (top solid line) with results of the count rate modeling (see text).

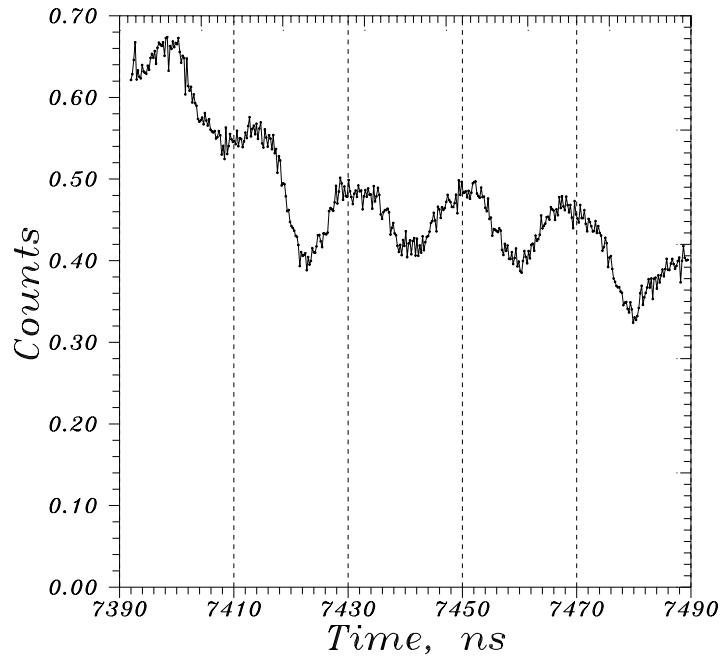


Figure 19: Proton losses of the same bunches as in Fig.17 during acceleration (at “parabola”).

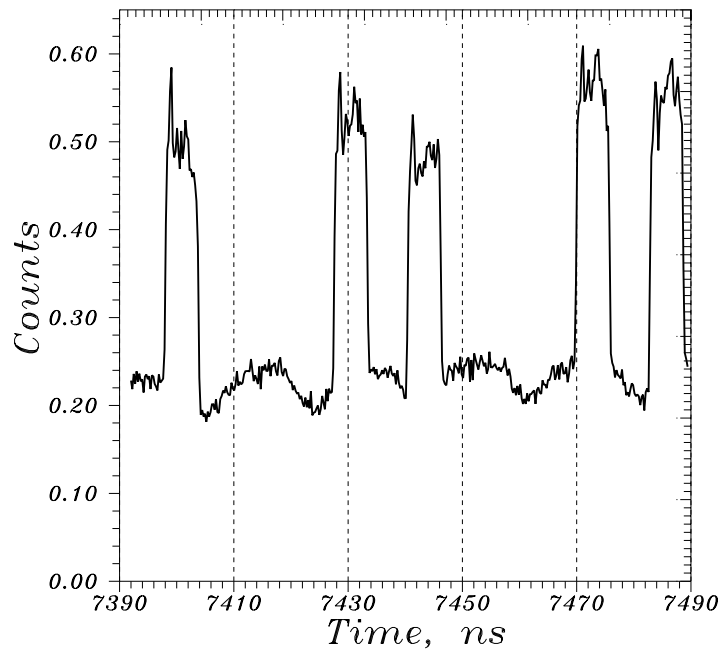


Figure 20: Proton losses of the same bunches as in Fig.17 at the top energy of 800 GeV.

## 5 Conclusion

We studied the structure of the proton losses in the Tevatron during fixed target operation with use of very fast Beam Loss Monitors based on PIN photodiodes. The BLM are very useful as they have huge dynamical range of more than  $10^8$ : from 0.1 Hz to few tens of MHz. Being very resistive to radiation, the PIN-BLMs are found very useful for accelerator applications. They allowed us to investigate the losses at the time scales from ten minutes to tens of nanoseconds, to observe the loss distribution over the whole Tevatron acceleration cycle, over one turn, one batch of bunches, and over few bunches.

These probes can be very useful for the Run II and TEV33 upgrades of the Tevatron collider. They can detect losses from different proton and antiproton bunches with minimum bunch spacing of 132 ns. The theory predicts that the losses will vary from bunch-to-bunch due to different bunch dynamics, therefore, the PIN-BLMs will provide the information needed for the beam control. For routine operation at Run II and TEV33, several probes can be installed in addition to an existing (much slower) loss monitoring system at the locations upstream and downstream of the collimators (that allows us to separate losses of protons and antiprotons, as it's done for electrons and positrons at LEP [14]), and at several other important locations.

### Acknowledgments

I am indebted to Jim Zagel and Marvin Olson for their practical help at the early stage of the studies and during installation of the probes at the Tevatron tunnel. I also acknowledge technical assistance of Rupe Crouch and Sasha Moibenko in developing the data acquisition system for the experiment. My sincerely gratitude to Kay Wittenburg (DESY) and Julien Bergoz (BERGOZ Co.) for some useful hints concerning the BLM operation, and Fernando Ridoutt (DESY) for cooperation in the probes calibration. Very useful discussions on the scheme and the results of these studies were held with Nikolay Mokhov, Sasha Drozhdin, Pat Colestock, Oleg Krivosheev, Mike Martens and Alan Hahn. I would like to thank Marvin Olson, Jim Zagel, Pat Smith and Stan Pruss for reading the manuscript and useful correction, and Dave Finley and John Marriner for their interest in this work and steady support.

### References

- [1] J.P.Marriner, "The Fermilab Proton-Antiproton Collider Upgrades", FERMILAB-Conf-96/391 (1996); S.D.Holmes, *et.al*, FNAL-TM-1920 (1995).
- [2] P.Bagley,*et. al*, "Summary of the TEV33 Working Group", FERMILAB-Conf-96/392 (1996).

- [3] V.Shiltsev, "On Crossing Angle at TEV33", FERMILAB-FN-653 (1997).
- [4] V.Shiltsev, D.Finley, "Electron Compression" of the Beam-Beam Footprint in Tevatron", FNAL-TM-2008 (1997).
- [5] D.Neuffer, "Discussion of Parameters, Lattices and Beam Stability for the MegaCollider", FERMILAB-TM-1964 (1995);  
G.W.Foster, E.Malamud, "Low-Cost Hadron Collider at Fermilab: A Discussion Paper", FERMILAB-TM-1976 (1996).
- [6] R.Shafer, *et.al.*, "The Tevatron Beam Position and Beam Loss Monitoring System", *Proc. 12th Int. Conf. On High-Energy Accel.*, Fermilab (1986), p.609.
- [7] E.Bleufler, R.O.Haxby, eds., "Methods of Experimental Physics: Vol.2, Electronic Methods", Part A, Academic Press, New York (1975);  
G.Charpak, F.Sauli, "High-Resolution Electronic Particle Detectors", in *Experimental Techniques in High Energy Physics*, T.Ferbel, ed., Addison-Wisley Publishing (1987).
- [8] K.Wittenburg, "Strahlverlustdetektoren fur den HERA Protonen-Ring", DESY-HERA 89-23 (1989); see also the same author in *Nucl. Instr. Meth. A270* (1988), p.56; *Proc. 1st DIPAC*, CERN (1993), p.11; *Nucl. Instr. Meth. A345* (1994), p.226.
- [9] "Beam Loss Monitor. User's Manual", BERGOZ Precision Beam Instrumentation (1996).
- [10] F.Ridoutt, "Das Ansprechvermogen Des PIN-Strahlstrommonitors", DESY PKTR-Note-91 (1993).
- [11] K.Werhheim, K.Wittenburg, "Radiation Resistance of Beam Loss Monitors", Internal Report DESY M-94-08 (1994).
- [12] M.Zeidel, "The Proton Collimation System of HERA", PhD Thesis, DESY 94-103 (1994); see also the same author DESY-HERA 93-04 (1993); and K.-H.Mess, M.Zeidel, "Collimators as Diagnostic Tools in the Proton Machine of HERA", *Nucl. Instr. Meth. A351* (1994), p.279.
- [13] V.Shiltsev, *et al.* "Measurements of Ground Motion and Orbit Motion at HERA", DESY HERA 95-06 (1995).
- [14] H.Burkhard, *et. al.*, "Beam Tails in LEP", *Proc. 1996 EPAC*, Barcelona, p.1152; and I.Reichel, H.Burkhardt, G.Roy, "Observation and Simulation of Beam Tails in LEP", *Proc. 1997 PAC*, Vancouver.